Antarct. Meteorite Res., **19**, 1–19, 2006

Experimental petrology of ancient lunar mare basalt Asuka-881757: Spinel crystallization as a petrologic indicator

Tomoko Arai[1]*, Hiroshi Takeda[2] and Masamichi Miyamoto[2]

[1]*Antarctic Meteorite Research Center, National Institute of Polar Research, Kaga 1-chome, Itabash-ku, Tokyo 173-8515*
[2]*Department of Earth and Planetary Science, The University of Tokyo, Hongo, Bunkyo-ku, Tokyo 113-0033*
**Corresponding author. E-mail: tomoko@nipr.ac.jp*

(Received April 18, 2006; Accepted July 31, 2006)

Abstract: The paucity of titanian chromites in lunar-meteorite basalt Asuka (A)-881757 is unusual compared to the general occurrence of co-existing chromites and ulvöspinels in the Apollo and Luna mare basalts. The unique spinel crystallization of A-881757 is expected to hold a key to elucidate the crystallization and cooling episodes of the basalt. In this study, we investigated the possible reason for the missing chromite by conducting isothermal and cooling experiments on the bulk-rock composition of A-881757 and discuss the petrogenesis of the ancient low-Ti mare basalt in light of spinel crystallization. A series of isothermal experiments showed the A-881757 basalt magma is not saturated with chromite under the expected lunar oxygen fugacity condition (IW~IW-1). A peritectic reaction among chromite, melt, and pyroxene is present for A-881757 basalt magma under the more oxidized condition which is one or two log unit higher than the lunar condition. The cooling experiment successfully reproduced the chromian ulvöspinels with similar compositions to those in A-881757. The result of the cooling experiments further implies that ulvöspinels solely crystallized from highly-fractionated interstitial melts in the late crystallization stage. The disparity in the crystallization of the liquidus chromite between the low-Ti and very low-Ti basalts might reflect the difference of bulk Cr_2O_3 concentration. The low liquidus temperature and the paucity of the liquidus olivine in A-881757 infer that the A-881757 basalt represents a liquid derived from near-surface fractionation processes. Chromites might possibly have been present during that near-surface fractionation episode prior to the eruption of the magma.

key words: Lunar meteorite, ancient basalt magmatism, ulvöspinel-chromite solid solution, peritectic reaction, fractional crystallization

1. Introduction

Chromian spinel has been known as a useful and important petrogenetic indicator in igneous and metamorphic rocks of the terrestrial planets because of systematic relationships among spinel chemistry, bulk-rock composition, cooling history, mineral assemblage, and geological process (*e.g.*, Irvine, 1965, 1967; Sack and Ghiorso, 1991). Spinels in the low-Ti (LT) and very low-Ti (VLT) lunar mare basalts among Apollo and Luna returned samples generally show a variety of compositional and textural varia-

tions, dominantly in the ternary system $FeCr_2O_4$ (chromite)–$FeAl_2O_4$ (hercynite)–Fe_2TiO_4 (ulvöspinel) (as reviewed by Papike and Cameron, 1976; Papike and Vaniman, 1978). The principal cationic substitution is represented by $Fe^{2+}+Ti^{4+}\leftrightarrow 2(Cr^{3+}, Al^{3+})$ with substantial substitution of Mg and Fe. Most spinels with the above chemical variations tend to occur as titanian chromites mantled by chromian ulvöspinels (*e.g.* Papike and Vaniman, 1978). Some spinels show discontinuous compositional variations between the two with a sharp boundary, indicating that later chromian ulvöspinel discontinuously precipitates onto the earlier titanian chromite without subsequent subsolidus equilibration. Others show gradational zonings from a core of titanian chromite toward a rim of chromian ulvöspinel, suggesting diffusive exchange between the two. These features imply continuous crystallization from titanian chromite to chromian ulvöspinel, or discontinuous crystallization of the two spinels, followed by diffusion between the two during subsolidus equilibration.

Based on the above compositional and textural characteristics of spinels in mare basalts, a solid solution with some miscibility gap was suspected between chromite and ulvöspinel (Kushiro and Haramura, 1971). Subsequently, several experimental studies were conducted to understand the phase relation in the system of $FeCr_2O_4$ (chromite)–$FeAl_2O_4$ (hercynite)–Fe_2TiO_4 (ulvöspinel) (Muan *et al*., 1971, 1972; Lipin and Muan, 1975; Schreifels and Muan, 1975; Shuart and Muan, unpublished data). A series of their experimental data revealed the presence of extensive miscibility gaps in the solid solution of hercynite and ulvöspinel in the temperature range 1000–1300°C (Fig. 7 of Muan *et al*., 1972 and Fig. 2 of Schreifels and Muan, 1975). Thermodynamic calculation based on these experimental results succeeded to further determine the miscibility gap for the lower temperature showing the appearance of miscibility gaps in the chromite–ulvöspinel solid solution at 800°C and 900°C (Fig. 3(a) of Sack and Ghiorso, 1991).

In the terrestrial layered basic intrusions (*i.e*., Bushveld, Stillwater, Muskox) and in basic volcanic rocks (*i.e*., Kilauea, Reunion), both chromite and titaniferrous magnetite occur as well as in the many low-Ti lunar mare basalts, in which ulvöspinel corresponds to titaniferrous magnetite under the lunar reduced condition. The chromite always crystallizes early in the cooling history, either alone or with olivine. However, it likely ceases to crystallize, resulting in subsequent differentiates without spinel until crystallization of titaniferous magnetite begins. This termination of the crystallization of early chromite was explained by possible reaction between spinel, liquid and pyroxene, which generates a chrome-bearing pyroxene and ceases spinel crystallization (Irvine, 1967). Such a reaction among early chromite, liquid and pyroxene was experimentally proved for terrestrial basalt compositions (Hill and Roeder, 1974).

Lunar meteorite Asuka (A)-881757 is a coarse-grained, Fe-enriched mare basalt (Yanai, 1991; Takeda *et al*., 1993), that crystallized at $\approx$3.9 Ga (Misawa *et al*., 1993), long before most other mare rocks (Nyquist and Shih, 1992). This rock has bulk-rock TiO_2 concentration slightly higher than very low-Ti (VLT) basalt (1.5 wt%) (*e.g*., Yanai and Kojima, 1991; Warren and Kallemeyn, 1993). Its coarse-grained texture and pyroxene exsolution of submicron to a few micron wide indicate that this basalt is an unusually slowly cooled mare basalt by the typical mare basalt standard and further implies its probable formation in lava ponds or shallow intrusions (Arai *et al*., 1996). A-881757 is also distinguished from any known lunar rocks due to the lowest $^{238}U/^{204}Pb$

(μ) value ($\mu = 10 \pm 3$; Misawa *et al*., 1993), which is much lower than those of the LT mare basalts ($\mu = 100$–300; Tatsumoto *et al*., 1971). This indicates that the source region of the A-881757 basalts is the least differentiated mantle regarding the U-Pb isotopic system, unlike other known mare basalt samples. Thus, A-881757 is an important clue to illuminate unprecedented aspects of the ancient mare volcanism.

Arai *et al*. (1996) presented results of detailed mineralogical study on the A-881757, emphasizing spinel and pyroxene as a valid petrogenesis indicator. Due to the coarse-grained nature, A-881757 is extremely heterogeneous in modal abundance among the polished thin sections: some include only pyroxene and plagioclase with no opaque minerals, while others include abundant (more than 10 vol%) opaque phases, such as ilmenite, chromian ulvöspinel and troilite. Note that A-881757 includes only chromian ulvöspinels without titanian chromites as confirmed by our own observation of three opaque-rich polished thin sections, as well as results of Yanai and Kojima (1991) and Warren and Kallemeyn (1993). These chromian ulvöspinels show compositional variations both within and among grains in one opaque-rich thin section (Arai *et al*., 1996). The absence of the titanian chromite and the variations in composition and texture of the chromian ulvöspinels in A-881757 are atypical, compared to the co-existing chromites and ulvöspinels in the majority of Apollo and Luna basalts. The unique spinel crystallization of A-881757 is expected to hold a key to elucidate the crystallization and cooling episodes of the basalt.

There are three possible reasons to explain the paucity of titanian chromite in A-881757 basalt: (1) A-881757 magma was never saturated with chromite, (2) both the titanian chromites and chromian ulvöspinels crystallized from the magma, the former was not found in the collected sample because of sampling bias due to the heterogeneity of the rock, or (3) early-crystallizing titanian chromites disappear by a peritectic reaction of liquid, chromite, and pyroxene, like the terrestrial layered basic intrusion (Hill and Roeder, 1974). In this study, we investigated the cause of the missing chromite by conducting crystallization experiment on the bulk-rock composition of A-881757 and discuss the petrogenesis of the ancient low-Ti mare basalt in light of the spinel crystallization.

2. Experimental procedure

Experiments were performed using synthetic starting materials of which compositions are nearly identical to that of A-881757 (Table 1). First, an oxide mixture of appropriate bulk composition with excess (~5 wt%) Fe was fused at 1300°C, well above the liquids temperature of the basaltic magma, for one hour under relatively reduced conditions ($fO_2 = 10^{-10}$ bar) in a platinum crucible, so that a platinum crucible may absorb Fe as much as possible. The glasses were subsequently fused for one hour to become homogenous at 1300°C, $fO_2 = 10^{-6}$ bar. After fusion, they were quenched in water, crushed using an agate mortar, and probed to ensure the homogeneity of glasses. Since the remarkable Fe loss was observed, the procedure stated above was repeatedly conducted with ~5 wt% additional FeO, until the composition comparable to that of A-881757 was attained.

All the experiments were conducted with a gas-mixing furnace at Department of

Table 1. Chemical compositions of synthetic starting material and bulk-rock A-881757 (wt%).

	Starting material	A-881757*
SiO_2	47.0	45.4
TiO_2	1.62	1.66
Al_2O_3	10.5	11.5
FeO	23.2	21.2
MnO	—	0.25
MgO	5.93	6.41
CaO	11.5	12.0
Na_2O	0.43	0.50
K_2O	—	0.04
Cr_2O_3	0.21	0.17
Total	100.5	99.1

* Yanai and Kojima (1991).

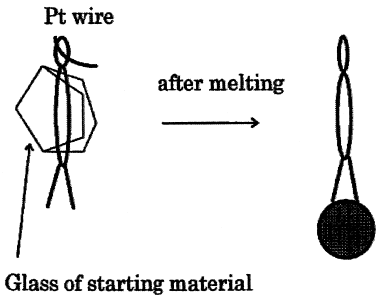

Fig. 1. A schematic figure showing that a synthetic starting material initially suspended by a Pt wire contacts with the Pt wire at two points after melting.

Earth and Planetary Science, the University of Tokyo, except several preliminary experiments undertaken at Institute for Study of the Earth's Interior, Okayama University. Oxygen fugacity was controlled by H_2-CO_2 gas mixtures and measured with a solid oxygen electrolytic zirconia cell (Miyamoto and Mikouchi, 1996). Experimental runs were conducted using 30 mg of the starting material suspended with $Pt_{87}Rh_{13}$ wire ($\varnothing$ = 0.1 mm) in the ceramic tube of the vertical gas-mixing furnace. Temperature was monitored by Pt-10Rh thermocouples calibrated against the melting point of gold. In order to minimize the loss of Fe from experimental charges, an approach illustrated in Fig. 1 was taken, where an experimental charge contacts with a Pt wire at two points once the charge is melted.

For both isothermal and cooling experiments, the charges were at first, held at 1200°C for two hours to obtain homogeneous melt without crystalline phases. The temperature of each isothermal run was attained by changing the vertical position of the suspended charge in the furnace, instead of changing the temperature of the furnace by changing the set point of the temperature controller. Since it takes times to attain a target temperature from the initial set point of 1200°C by the controller, such an ap-

proach would lead to relatively slow cooling rates for the isothermal experiment. The temperature gradient along the different vertical direction in the furnace was measured in advance. Oxygen fugacity was changed depending on the temperature at which the isothermal experimental run was undertaken.

Isothermal runs were performed at temperatures of 1200, 1180, 1160, 1140, 1120, 1100, 1075, and 1050°C, and under oxygen fugacities of Magnetite-Wüstite (MW), Iron-Wüstite (IW)+1, IW, IW-1 buffers. The duration of the isothermal run was one day for temperatures higher than 1100°C, and two days below 1100°C, which were determined based on the time study to survey the time (run duration) dependency of compositions of the minerals and glasses (Table 2). Time studies were performed for 1, 2 and 6 days to assess the equilibrium at 1050°C that is the lowest temperature of the experiment.

Cooling experiments were performed over the temperature range from 1200°C to 1050°C with three different cooling rates, 3°C/hr, 6°C/hr, and 300°C/hr, and three different redox conditions with constant CO_2/H_2 ratio, starting from $\log fO_2 = -12.9$ bar (IW-1 buffer at 1200°C), −10.9 (IW+1 at 1200°C), and −9.1 (MW at 1200°C) respectively. Since all the runs were conducted under the constant CO_2/H_2 ratios, the oxygen fugacity at a given temperature becomes lower than the respective buffer curve as the temperature decreases. As a result, the oxygen fugacity conditions at 1050°C were lower than the buffer curves, by 0.2 log unit at MW buffer, 0.9 log unit at IW+1, and 0.5 log unit at IW-1. The condition and the results of isothermal and cooling experiments are tabulated in Tables 3 and 4. Analyses of phase compositions were done by a JEOL JXA-733 electron probe microanalyzer (EPMA) at the Ocean Research Institute, and a JEOL JXA-8600 Super Probe at Department of Earth and Planetary Science, University of Tokyo. All mineral analyses were done using wavelength dispersive spectrometers operating 15 kV accelerating voltage, a 12 nA beam current and a focused beam. A combination of silicate and oxide mineral standards was used for calibration of silicates and oxides.

Table 2. Chemical compositions of minerals and glasses (wt%) for time studies.*

	Glass			Pyroxene			Plagioclase		
	1 day	2 days	6 days	1 day	2 days	6 days	1 day	2 days	6 days
SiO_2	48.8	48.6	48.2	49.9	50.7	50.4	49.0	48.4	47.4
TiO_2	1.7	1.8	1.8	0.4	0.3	0.3	—	—	—
Al_2O_3	10.7	10.8	10.4	1.9	1.8	1.8	31.0	31.8	32.6
FeO	22.5	23.7	24.0	24.6	24.8	25.8	1.4	1.1	1.1
MgO	3.4	3.5	3.6	15.6	15.7	15.4	0.3	0.3	0.2
CaO	10.8	10.9	10.8	5.8	6.0	5.5	17.2	17.3	17.8
Na_2O	0.4	0.5	0.4	nd	nd	nd	nd	nd	nd
Cr_2O_3	0.2	0.2	0.2	0.4	0.4	0.5	0.0	0.0	0.0
Total	98.3	99.8	99.2	98.7	99.7	99.9	100.5	100.8	100.4

* Time studies were conducted at $T = 1050$°C under $\log fO_2 = IW+1$.
nd = not detected.

Table 3. Experimental conditions and products of isothermal experiments.

Run No.	T (℃)	log fO_2 (bar)	Duration (hr)*	Phases present¶	Run No.	T (℃)	log fO_2 (bar)	Duration (hr)*	Phases present¶
21	1200	MW	24	Gl	22	1120	MW	25	Gl+Sp+Px
9	1200	IW+2	24	Gl	23	1120	IW+2	25	Gl+(Px)§
7	1200	IW+1	24	Gl	24	1120	IW+1	24	Gl+Px+Ol
8	1200	IW	24	Gl	25	1120	IW	24.5	Gl+Px
10	1200	IW-1	24	Gl	26	1120	IW-1	25	Gl+Px
27	1180	MW	24	Gl	36	1100	MW	24	Gl+Sp+Px
28	1180	IW+2	25	Gl	35	1100	IW+2	24	Gl+Sp+Px
29	1180	IW+1	24	Gl	34	1100	IW+1	24	Gl+Px
30	1180	IW	24	Gl	33	1100	IW	24	Gl+Px
31	1180	IW-1	26	Gl	32	1100	IW-1	24.5	Gl+Px
14	1160	MW	25	Gl+Sp	52	1075	MW	50	Gl+Sp+Px
13	1160	IW+2	25	Gl+Sp	60	1075	IW+2	50	Gl+Sp+Px
12	1160	IW+1	25	Gl	55	1075	IW+1	50	Gl+Px
11	1160	IW	26	Gl	57	1075	IW	50	Gl+Px
15	1160	IW-1	24	Gl	56	1075	IW-1	50	Gl+Px+Pl+Fe
16	1140	MW	24	Gl+Sp+Px	51	1050	MW	50	Gl+Sp+Px+Pl
17	1140	IW+2	24	Gl+Sp	59	1050	IW+2	50	Gl+Px+Pl
18	1140	IW+1	24	Gl+Px	46	1050	IW+1	50	Gl+Px+Pl
19	1140	IW	24	Gl+Px	61	1050	IW	50	Gl+Px+Pl
20	1140	IW-1	24	Gl+Px	50	1050	IW-1	50	Gl+Px+Pl

* Except experiments at 1200℃, all the experimental charges were once held at 1200℃ for 2 hours to obtain homogeneous melt.

¶ Gl: Glass, Sp: Spinel, Ol: Olivine, Px: Pyroxene, Pl: Plagioclase, Fe: Metallic Fe.

§ Bad stoichiometry and total wt%.

Table 4. Experimental conditions and products of cooling experiments.

Run No.	Start		End		Cooling rate (℃/hr)	Phases present¶
	T* (℃)	log fO_2 (bar)	T (℃)	log fO_2§ (bar)		
5	1200	−9.10 (MW)	1050	−11.8	6	Gl+Px+Pl+Sp
2	1200	−10.9 (IW+1)	1050	−13.9	6	Gl+Px+Pl
1	1200	−12.9 (IW-1)	1050	−15.5	6	Gl+Px+Pl+Fe
4	1200	−10.9 (IW+1)	1050	−13.9	3	Gl+Px+Pl
3	1200	−12.9 (IW-1)	1050	−15.5	3	Gl+Px+Pl+Fe+Si
39	1200	−10.9 (IW+1)	1050	−13.9	300	Gl+Px+Pl+Sp
37	1200	−12.9 (IW-1)	1050	−15.5	300	Gl+Px+Pl+Si

* All the experimental charges were once held at 1200℃ for 2 hours to obtain homogeneous melt prior to cooling.

§ Since all the runs were conducted under the constant CO_2/H_2 ratios, the oxygen fugacity at a given temperature becomes lower than the respective buffer curve as the temperature decreases. As a result, the oxygen fugacity conditions at 1050℃ were lower than the buffer curves, by 0.2 log unit at MW buffer, 0.9 log unit at IW+1, and 0.5 log unit at IW-1.

¶ Gl: Glass, Sp: Spinel, Px: Pyroxene, Pl: Plagioclase, Fe: Metallic Fe, Si: Silica mineral.

3. Results

3.1. Isothermal experiments

Phases present in the isothermal experiments are plotted on the temperature (°C) *vs.* logarithmic fO_2 (bar) (Fig. 2). Chemical compositions of glasses and minerals present are shown in Tables 5–8. Above 1180°C, no crystals appeared over the entire range of the oxygen fugacity. At 1160°C, MW and IW+2, aluminous chromite crystallized as a liquidus phase. It is to be noted that the aluminous chromites disappear between 1140–1075°C and then reappear at 1075°C under IW+2, whereas they continuously crystallized with lowering temperatures under MW. Under lower oxygen fugacities (IW+1, IW, and IW-1), pyroxene is the liquidus phase at 1140°C. Pyroxene joined with aluminous chromite at 1140°C under MW as well. A small amount of olivine is found at IW+1, T=1120°C and at IW+2, T=1100°C. Plagioclase joined at 1075°C under fO_2=IW-1 and at 1050°C under the rest of the oxygen fugacities.

Crystal sizes of the spinels are 10 μm or less. Almost all the aluminous chromite shows neither good total wt% (92–97 wt%) nor good stoichiometry (18.5–18.8 of total

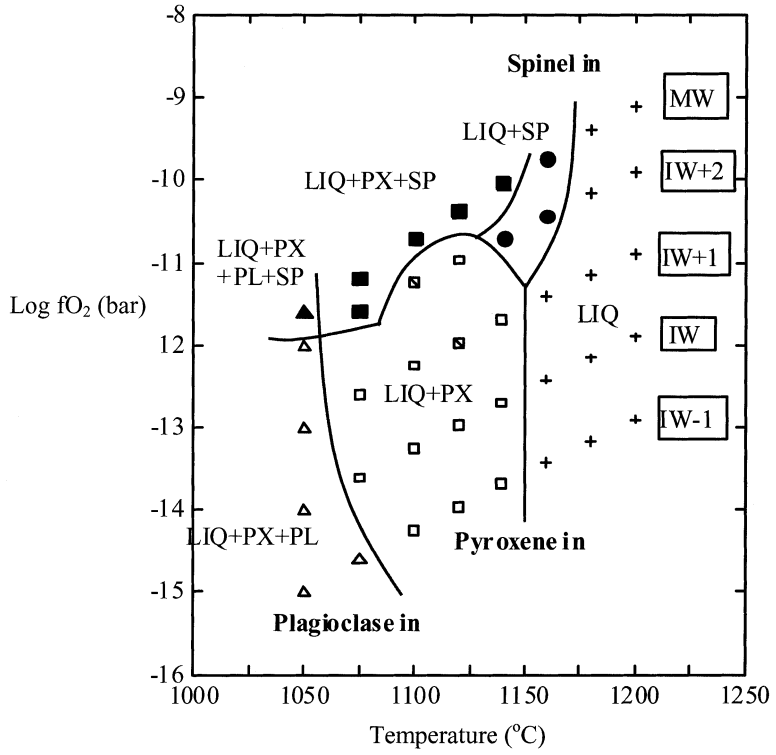

Fig. 2. Oxygen fugacity vs. temperature diagram, illustrating the phase assemblages and their stability fields for A-881757 basalt composition. Each line and curve depicts the effect of oxygen fugacity on the temperature of first appearance or liquidus of a separate phase. The peritectic reaction of chromite, melt, and pyroxene is shown by the disappearance of spinel between 1140–1075°C under IW+2. LIQ: liquid, SP: spinel, PX: pyroxene, PL: plagioclase.

cation to 24 oxygen). This would be partly because all spinels that crystallized around MW buffer contain significant amount of Fe^{3+}. As a result, these chromites probably include a magnetite component. The result of calculation of spinel formula indicates

Table 5. Chemical compositions (wt%) of glasses in isothermal experiments.

	1200 °C					1180 °C				
	MW	IW+2	IW+1	IW	IW-1	MW	IW+2	IW+1	IW	
SiO_2	48.7	49.1	49.3	49.8	48.7	49.7	49.4	49.4	49.6	
TiO_2	1.5	1.5	1.6	1.6	1.6	1.6	1.6	1.5	1.5	
Al_2O_3	9.3	9.6	10.2	9.7	10.3	9.7	9.9	9.8	9.9	
FeO	22.9	21.6	20.5	21.3	20.4	21.5	21.5	21.5	21.7	
MgO	5.4	5.5	5.7	5.6	6	5.5	5.4	5.4	5.5	
CaO	10.3	10.6	10.7	10.3	11.1	10.3	10.4	10.3	10.3	
Na_2O	0.4	0.4	0.4	0.3	0.3	0.4	0.4	0.4	0.4	
Cr_2O_3	0.2	0.2	0.2	0.2	0.2	nd	nd	0.2	0.2	
Total	98.7	98.5	98.6	98.8	98.6	98.7	98.6	98.5	99.1	
	1160 °C					1140 °C				
	MW	IW+2	IW+1	IW	IW-1	MW	IW+2	IW+1	IW	IW-1
SiO_2	48.8	49.6	49.4	49.2	48.7	49.3	49.5	49.7	49.4	49.2
TiO_2	1.5	1.5	1.6	1.5	1.6	1.5	1.6	1.6	1.6	1.6
Al_2O_3	9.8	9.9	10.0	9.8	10.7	10.0	9.8	10.2	10.1	10.7
FeO	22.6	22.4	21.0	22.2	21.3	22.8	22.1	22.1	21.4	21.4
MgO	5.8	5.5	5.6	5.7	6.0	5.2	5.4	4.9	4.9	4.7
CaO	10.2	10.2	10.4	10.3	11.1	10.3	10.2	10.6	10.5	11.1
Na_2O	0.4	0.4	0.4	0.4	0.3	0.4	0.4	0.3	0.4	0.4
Cr_2O_3	nd	nd	nd	0.2	0.2	nd	nd	nd	nd	nd
Total	99.1	99.5	98.4	99.3	99.9	99.5	99.0	99.4	98.3	99.1
	1120 °C					1100 °C				
	MW	IW+2	IW+1	IW	IW-1	MW	IW+2	IW+1	IW	IW-1
SiO_2	49.7	49.4	48.8	49.7	49.1	48.8	50.1	49.4	50.0	49.7
TiO_2	1.6	1.6	1.6	1.7	1.7	1.6	1.6	1.7	1.7	1.7
Al_2O_3	10.0	9.8	10.3	10.5	10.8	10.6	10.9	10.6	10.6	11.4
FeO	22.5	21.8	22.5	22.0	21.5	22.7	21.4	21.5	21.1	21.0
MgO	4.4	5.4	4.3	4.2	4.0	3.8	3.7	4.3	4.4	4.0
CaO	10.3	10.2	10.5	10.8	11.1	10.5	10.5	10.8	10.8	11.5
Na_2O	0.5	0.4	0.4	0.5	0.4	0.5	0.4	0.4	0.4	0.4
Cr_2O_3	nd	nd	nd	nd	nd	nd	nd	nd	nd	nd
Total	99.0	98.6	98.4	99.4	98.6	98.5	98.6	98.7	99.0	99.7
	1075 °C					1050 °C				
	MW	IW+2	IW+1	IW	IW-1	MW	IW+2	IW+1	IW	IW-1
SiO_2	49.4	49.3	49.4	48.9	49.4	47.8	48.8	49.1	48.7	50.2
TiO_2	1.7	1.8	1.8	1.7	1.7	2.0	2.0	1.9	2.0	1.9
Al_2O_3	10.8	11.0	11.0	11.1	11.3	10.8	10.6	10.8	10.1	10.7
FeO	22.7	22.5	21.8	22.5	21.8	24.9	24.4	22.6	24.0	22.1
MgO	3.4	3.4	3.6	3.7	3.5	3.2	2.9	3.7	2.9	3.5
CaO	11.0	11.1	11.0	11.0	11.0	10.3	10.2	10.9	10.5	10.9
Na_2O	0.5	0.5	0.5	0.5	0.5	0.5	0.4	0.5	0.4	0.4
Cr_2O_3	nd	nd	nd	nd	nd	nd	nd	nd	nd	nd
Total	99.5	99.6	99.1	99.4	99.2	99.5	99.3	99.5	98.6	99.7

nd = not detected.

Table 6. Chemical compositions of spinels in isothermal experiments.

	1160 °C	1140 °C	1120 °C	1100 °C	1075 °C
wt%	MW	IW+2	MW	MW	MW
SiO_2	0.1	0.2	0.6	0.2	0.2
TiO_2	2.9	3.3	5.2	5.0	4.8
Al_2O_3	10.6	10.9	11.5	10.5	11.3
FeO	34.9	40.0	43.9	44.7	43.0
MgO	4.2	4.4	3.7	3.2	3.1
CaO	0.3	0.4	0.4	0.3	0.3
Cr_2O_3	42.5	36.8	31.6	32.0	31.9
Total	95.5	96.0	96.9	95.9	94.6
molar					
Fe/(Fe+Mg)	0.82	0.83	0.87	0.89	0.89
Ti/(Ti+Cr)	0.06	0.08	0.13	0.13	0.13
$FeCr_2O_4$	0.55	0.51	0.44	0.45	0.45
$FeAl_2O_4$	0.22	0.23	0.24	0.22	0.24
Fe_2TiO_4	0.08	0.09	0.14	0.13	0.13
Fe_3O_4	0.15	0.17	0.18	0.19	0.17

Table 7. Chemical compositions of pyroxenes in isothermal experiments.

	1140 °C				1120 °C				1100 °C				
wt%	MW	IW+1	IW	IW-1	MW	IW+1	IW	IW-1	MW	IW+2	IW+1	IW	IW-1
SiO_2	51.6	52.3	52.2	52.3	51.5	51.1	51.7	51.8	50.4	50.1	51.2	51.1	51.6
TiO_2	0.3	0.2	0.2	0.3	0.3	0.3	0.3	0.3	0.3	0.3	0.3	0.3	0.4
Al_2O_3	1.2	1.2	1.0	1.1	1.6	1.8	1.6	1.5	1.8	1.7	1.6	1.3	1.6
FeO	22.7	22.9	23.7	22.5	24.6	24.7	24.4	23.8	24.6	24.9	24.4	24.3	23.3
MgO	19.5	19.4	19.1	19.5	17.8	17.1	17.4	17.7	16.2	16.3	16.9	17.6	17.9
CaO	3.5	3.4	3.2	3.6	3.6	3.9	4.3	4.3	5.0	4.8	4.8	4.4	4.6
Cr_2O_3	0.6	0.5	0.4	0.3	0.6	0.6	0.6	0.4	0.5	0.3	0.6	0.4	0.4
Total	99.4	99.9	99.8	99.6	100	99.5	100.3	99.8	98.8	98.4	99.8	99.4	99.8
molar													
Fe/(Fe+Mg)	0.40	0.40	0.41	0.39	0.44	0.45	0.44	0.43	0.46	0.46	0.45	0.44	0.42
Ti/(Ti+Cr)	0.32	0.28	0.32	0.49	0.32	0.32	0.32	0.42	0.36	0.49	0.32	0.42	0.49
Wo	0.07	0.07	0.07	0.07	0.08	0.08	0.09	0.09	0.11	0.10	0.10	0.09	0.10
Fs	0.37	0.37	0.38	0.36	0.40	0.41	0.40	0.39	0.41	0.41	0.40	0.40	0.38
En	0.56	0.56	0.55	0.56	0.52	0.51	0.51	0.52	0.48	0.48	0.50	0.51	0.52

	1075 °C					1050 °C				
wt%	MW	IW+2	IW+1	IW	IW-1	MW	IW+2	IW+1	IW	IW-1
SiO_2	51.3	50.3	51.0	52.3	50.9	49.5	49.6	50.7	49.6	50.0
TiO_2	0.3	0.4	0.4	0.3	0.4	0.3	0.4	0.3	0.4	0.5
Al_2O_3	2.1	2.0	2.2	1.1	2.4	1.7	1.9	1.8	1.9	1.9
FeO	25.0	24.8	24.9	22.5	24.5	26.2	26.2	24.8	26.4	24.8
MgO	16.4	15.9	16.1	19.5	16.9	13.7	13.5	15.7	13.6	14.8
CaO	4.8	5.5	5.2	3.6	4.3	6.9	7.1	6.0	6.9	7.1
Cr_2O_3	0.5	0.6	0.5	0.3	0.5	0.4	0.3	0.4	0.2	0.3
Total	100.4	99.5	100.3	99.6	99.9	98.7	99.0	99.7	99.0	99.4
molar										
Fe/(Fe+Mg)	0.46	0.47	0.46	0.39	0.45	0.52	0.52	0.47	0.52	0.48
Ti/(Ti+Cr)	0.36	0.39	0.43	0.49	0.43	0.42	0.56	0.42	0.66	0.61
Wo	0.10	0.12	0.11	0.07	0.09	0.15	0.15	0.13	0.15	0.15
Fs	0.41	0.41	0.41	0.36	0.41	0.44	0.44	0.41	0.44	0.41
En	0.48	0.47	0.48	0.56	0.50	0.41	0.41	0.46	0.41	0.44

Wo = Ca/(Ca+Fe+Mg), Fs = Fe/(Ca+Fe+Mg), En = Mg/(Ca+Fe+Mg).

Table 8. Chemical compositions (wt%) of plagioclases in isothermal experiments.

	1075 °C	1050 °C				
	IW-1	MW	IW+2	IW+1	IW	IW-1
SiO_2	48.8	48.2	48.6	48.4	48.5	47.8
Al_2O_3	31.6	31.6	31.2	31.8	31.7	31.6
FeO	1.0	1.3	1.4	1.1	1.2	1.1
MgO	0.3	0.3	0.2	0.3	0.3	0.3
CaO	17.5	17.0	17.0	17.3	17.0	17.2
Na_2O	1.1	1.3	1.3	1.4	1.4	1.2
Total	100.3	99.7	99.7	100.3	100.1	99.2
An	0.90	0.88	0.88	0.87	0.87	0.89

An = Ca/(Ca+Na) mol.

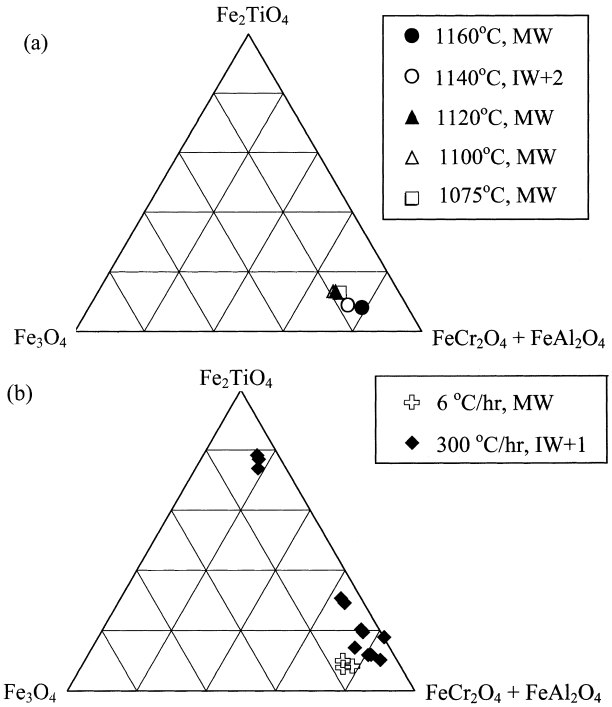

Fig. 3. Spinel compositions in the isothermal and cooling experiments projected in a ternary diagram of Fe_2TiO_4 (ulvöspinel)–[$FeCr_2O_4$ (chromite) + $FeAl_2O_4$ (hercynite)]–Fe_3O_4 (magnetite). (a) Isothermal experiments and (b) cooling experiments.

that these spinels contain 15 mol% of magnetite component (Table 6). Some chromite apparently include high concentration of SiO_2 due to their small (mostly <10 μm) crystal size, causing electron beam overlapping of spinels with pyroxenes enclosing them. The spinels from each run are projected on the Fe_2TiO_4 (ulvöspinel)–[$FeCr_2O_4$ (chromite) + $FeAl_2O_4$ (hercynite)]–Fe_3O_4 (magnetite) ternary diagram (Fig. 3a). Chromite compositions in all the runs are relatively similar. However, there seems to be a tendency that the chromites crystallizing at higher temperatures are slightly enriched in magnetite component and depleted in ulvöspinel component, though the compositional variation

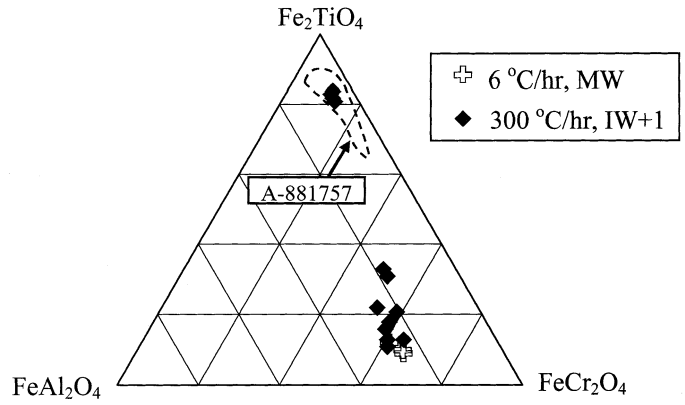

Fig. 4. Spinel compositions of the cooling experiments projected in a ternary diagram of Fe_2TiO_4 (ulvöspinel)–$FeCr_2O_4$ (chromite)–$FeAl_2O_4$ (hercynite), in comparison with those in A-881757 from Arai et al. (1996), which is shown with the range enclosed by the dotted line.

occurs only within a small range.

3.2. Cooling experiments

For all cooling runs, dendritic pyroxenes and plagioclases are observed. In a run with cooling rate of 6°C/hr starting with MW at 1200°C, aluminous chromites are present with pyroxene and plagioclase (run No. 5 of Table 4). Their crystal sizes are by far less than 10 μm and quite difficult to get good-quality compositional data. The compositions are analogous to those of isothermal runs under MW. In a run with cooling rate of 300°C/hr starting with IW+1 at 1200°C, Al and Ti-bearing chromites, and chromian ulvöspinels are present (run No. 6 of Table 4). Chromites which are relatively small (up to 10 μm) and sub-rounded, are enclosed by pyroxenes, up to 1 mm in size (Fig. 5a). In contrast, chromian ulvöspinels, which are larger (up to 20 μm) and euhedral, crystallize at the grain boundaries of pyroxene and plagioclase or in the interstitial glass (Fig. 5b). The interstitial glasses where chromian ulvöspinels precipitated contain ~5.0 wt% of TiO_2. Mineral compositions of these spinels are shown in Table 9 and Fig. 3b. Both the Al, Ti-bearing chromites and chromian ulvöspinels show grain-to-grain compositional variations. Note that the compositions of the chromian ulvöspinels are almost identical to those observed in A-881757 with regard to the ternary system of Fe_2TiO_4 (ulvöspinel)–$FeCr_2O_4$ (chromite)–$FeAl_2O_4$ (hercynite) (Fig. 4), though they contain 6–8 wt% of magnetite component (Fe_3O_4), unlike those in A-881757. A compositional hiatus between the Al and Ti-bearing chromites and the Cr and Ti-bearing ulvöspinels is also noticeable (Fig. 4). A chromite mantled with ulvöspinel reproduced by cooling experiments on Apollo 12 low-Ti mare basalt by Lofgren *et al.* (1974) was not found in this experiment.

No spinel crystallized, both at the more slowly cooled experiments starting at IW+1 and IW-1, and at rapidly cooled experiments starting at IW-1. Ilmenite is not found in any experimental products although it is one of main opaque minerals in A-881757. This is probably because the interstitial liquid where ulvöspinel crystallized would not

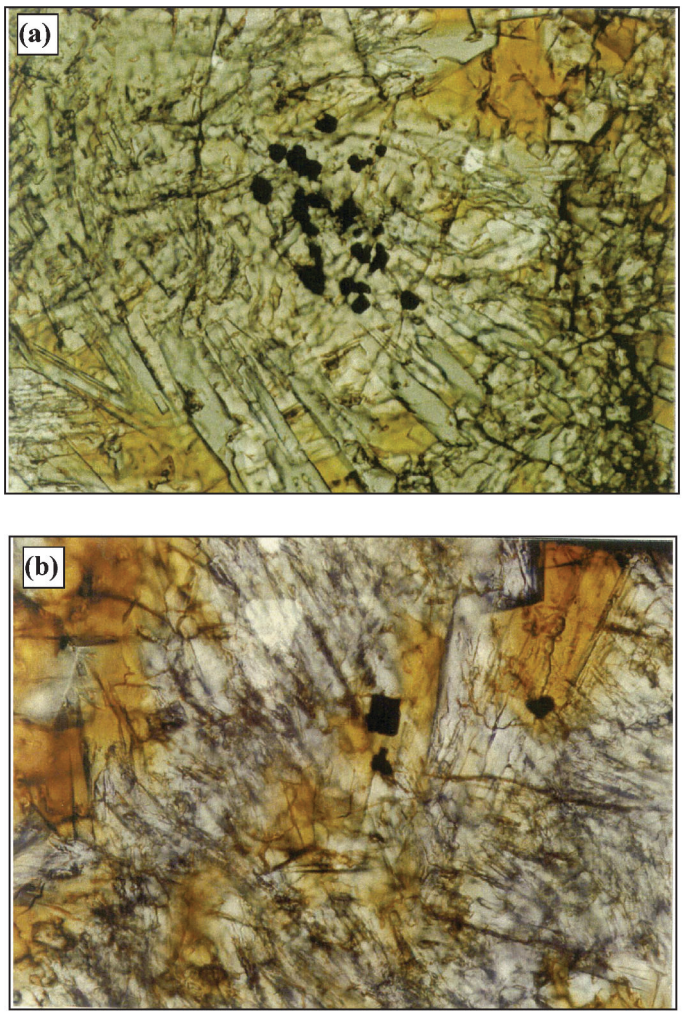

Fig. 5. Photomicrographs of crystallized spinels in the cooling experiment (run no. 6 of Table 4) with a cooling rate of 300°C/hr starting at $fO_2 = IW + 1$. Field of views is 330 μm. (a) Sub-rounded titanian chromite crystals (black) enclosed in dendritic pyroxenes (pale green), (b) chromian ulvöspinel (black) crystallized in the interstitial melt (brown).

be saturated with ilmenite yet. Also in the isothermal experiments of Apollo low-Ti basalts (Walker *et al*., 1976, 1977), ilmenite does not crystallize, which is probably due to the same reason.

4. Discussion

4.1. Phase relation of A-881757 basalt magma

Chromite was a liquidus phase only at MW and IW+2, which are more oxidized than the expected lunar condition (IW–IW-1) (Sato *et al*., 1973). This implies that the

Table 9. Chemical compositions of spinels in cooling experiments.

wt%	Run #5 (6 °C/hr, MW)				Run #39 (300 °C/hr, IW+1)						
SiO_2	0.4	0.5	0.4	0.3	0.2	0.1	0.1	0.2	0.1	0.4	0.8
TiO_2	3.0	2.9	3.7	3.4	7.0	4.5	3.9	4.6	7.4	5.5	5.3
Al_2O_3	9.8	9.7	10.4	11.1	11.9	10.2	12.8	12.3	9.4	9.9	10.9
FeO	40.1	37.8	42.6	39.7	37.6	39.6	37.5	39.0	41.5	38.2	41.1
MgO	2.2	4.6	1.9	4.5	1.4	1.3	1.7	1.9	1.3	1.4	1.3
CaO	0.3	0.8	0.4	0.5	0.2	0.3	0.4	0.3	0.3	0.3	0.5
Cr_2O_3	39.0	38.5	36.0	34.8	43.3	41.6	42.1	40.1	39.9	35.6	36.0
Total	94.9	94.8	95.4	94.3	101.5	97.6	98.5	98.4	99.9	91.3	95.9
molar											
Fe/(Fe+Mg)	0.91	0.82	0.93	0.83	0.94	0.95	0.93	0.92	0.95	0.94	0.95
Ti/(Ti+Cr)	0.07	0.07	0.09	0.08	0.13	0.09	0.08	0.10	0.15	0.13	0.12
$FeCr_2O_4$	0.57	0.55	0.52	0.49	0.59	0.59	0.58	0.56	0.56	0.54	0.52
$FeAl_2O_4$	0.21	0.21	0.22	0.23	0.24	0.21	0.26	0.25	0.20	0.22	0.23
Fe_2TiO_4	0.08	0.08	0.10	0.09	0.18	0.12	0.10	0.12	0.20	0.16	0.14
Fe_3O_4	0.14	0.17	0.16	0.18	0.00	0.08	0.05	0.07	0.05	0.08	0.10

wt%	Run #39 (300 °C/hr, IW+1)									
SiO_2	0.1	0.2	0.4	0.2	0.2	0.8	0.2	0.1	0.1	0.1
TiO_2	7.6	10.8	11.3	9.8	20.4	18.7	26.5	27.9	28.1	28.5
Al_2O_3	11.3	8.0	8.1	7	3.2	3.7	2.6	2.4	2.3	2.5
FeO	41.3	43.5	44.1	44.9	52.0	53.9	58.6	59.2	58.9	59.9
MgO	1.3	1.3	1.4	1.2	1.2	1.3	1.3	1.3	1.3	1.3
CaO	0.3	0.4	0.3	0.3	0.3	0.5	0.4	0.3	0.3	0.3
Cr_2O_3	36.0	33.4	31.9	28.8	15.8	15.1	8.2	7.7	7.0	6.9
Total	97.9	97.6	97.5	92.2	93.1	94.0	97.8	98.9	98.0	99.5
molar										
Fe/(Fe+Mg)	0.95	0.95	0.95	0.95	0.96	0.96	0.96	0.96	0.96	0.96
Ti/(Ti+Cr)	0.17	0.23	0.25	0.25	0.55	0.54	0.76	0.78	0.79	0.80
$FeCr_2O_4$	0.51	0.48	0.46	0.44	0.24	0.23	0.12	0.11	0.10	0.10
$FeAl_2O_4$	0.24	0.17	0.17	0.16	0.07	0.08	0.06	0.05	0.05	0.05
Fe_2TiO_4	0.20	0.29	0.31	0.28	0.60	0.54	0.74	0.77	0.78	0.78
Fe_3O_4	0.05	0.06	0.06	0.12	0.09	0.15	0.08	0.06	0.06	0.06

A-881757 basalt magma is not saturated with chromite under equilibrium conditions. Studies of Cr partitioning among spinel, olivine and silicate liquid at the lunar oxygen fugacities below IW buffer showed that Cr^{2+} was the dominant Cr species in the lunar lavas (Akella *et al.*, 1976; Huebner *et al.*, 1976; Sato, 1978). It has been also reported that the ratio of $Cr^{3+}/(Cr^{3+}+Cr^{2+})$ in the melt systematically decreases with decreasing oxygen fugacity from QFM to IW buffer (Schreiber and Haskin, 1976; Barnes, 1986; Hanson and Jones, 1997). The absence of the chromite at lower oxygen fugacity conditions in this experiment is consistent with the above systematic variation of oxidation state of Cr with the oxygen fugacity. Since only Cr^{3+} can enter the octahedral site of the spinel structure, the $Cr^{3+}/(Cr^{3+}+Cr^{2+})$ value was probably not high enough for chromite crystallization under the lower oxygen fugacity such as around IW buffer.

The oxidation state of Fe also affects the spinel crystallization. Because the pres-

ence of Fe^{3+} expands the field of crystallization of spinel, the lack of Fe^{3+} at the lunar oxygen fugacity of IW~IW-1 effectively prevents spinel crystallization, which is consistent with the lack of chromites around IW.

The termination of the aluminous chromite within the temperature range of 1140°C–1075°C under IW+2 indicates the presence of a peritectic reaction among chromite, melt, and pyroxene for the A-881757 basalt composition at the oxygen fugacity around IW+2. This provides the evidence for the reaction among chromite, melt, and pyroxene in the lunar basalt composition and expands the study of the terrestrial basalts (Hill and Roeder, 1974). However, the oxygen fugacity of IW+2 is higher than the expected lunar redox condition (IW–IW-1 buffer) and is not readily applicable to the case for A-881757 magma.

4.2. Crystallization of A-881757 basalt and petrogenetic implication

Ulvöspinel is found together with chromite only in a cooling experiments with a very rapid cooling rate (300°C/hr) starting at IW+1 and ending at close to IW due to the constant CO_2/H_2 ratio during the cooling (see detail in the experimental procedure). The chemical composition and grain-to-grain compositional variation of the chromian ulvöspinel are similar to those of chromian ulvöspinels in A-881757 (Arai *et al*., 1996). This reveals that the ulvöspinels in A-881757 could be generated as a result of fractional crystallization during rapid cooling. The ulvöspinel crystallizes in the interstices between pyroxene and plagioclase in the run product, while the chromite occurs as inclusions of pyroxenes. This texture indicates that the ulvöspinel apparently crystallizes later than the chromite. Since A-881757 is low in titanium (1.6 wt% TiO_2), ulvöspinels could crystallize only from a highly fractionated melt that is locally enriched in TiO_2, such as trapped interstitial melts between pre-crystallizing pyroxene and plagioclase. In fact, the TiO_2 content of the interstitial melt where ulvöspinels crystallize reaches up to 5.0 wt%. The grain-to-grain compositional variations of ulvöspinels probably reflect the variation in the TiO_2 concentration among the highly-fractionated trapped interstitial melts.

In contrast, the presence of sub-rounded titanian chromites enclosed in the pyroxenes is enigmatic. Since the redox condition for the A-881757 basalt is expected somewhere around IW–IW-1, the titanian chromite in the cooling experiment at IW+1 is unlikley to represent a possible chromite crystallization in the A-881757 composition. Considered that the spinel was found only at higher oxygen fugacity than IW+2 in the isothermal experiments (Fig. 2), it is more natural to interpret that the presence of the titanian chromite is probably attributed to the extended stability field of the spinel to a slightly lower oxygen fugacity down to IW+1. Thus, the chromites would never have precipitated in the A-881757 magma during the entire crystallization sequence, with only ulvöspinels crystallizing at the later stage of fractionation.

Since the slower cooling rate (3–6°C/hr) failed to generate the spinels, A-881757 basalt may have been cooled as rapidly as typical mare basalts (~several tens°C/hr) (Taylor *et al*., 1991), or possibly even faster, with regards to the spinel crystallization. On the other hand, the lack of ulvöspinel in the cooling experiment at 300°C/hr starting at IW-1 can be attributed to the oxygen fugacity condition too low for the ulvöspinel stability (IW–0.5) (Sato *et al*., 1973).

4.3. Effect of Cr content on chromite crystallization

Several experimental studies on the terrestrial basalts have revealed that the crystallization of chromite or magnetite-ulvöspinel from basaltic liquids in near-surface environments is a function of combined effects of oxygen fugacity, temperature, melt composition, and co-crystallizing phases such as pyroxenes (*e.g.*, Hill and Roeder, 1974; Fisk and Bence, 1979). As discussed in Section 4.1, it has been experimentally demonstrated that the extent of the spinel stability field is very sensitive to small changes in the amount of chromium in the liquid (Hill and Roeder, 1974; Schreiber and Haskin, 1976; Barnes, 1986). This is because Cr^{3+} is extremely insoluble in silicate liquids and is strongly concentrated in spinel relative to other trivalent cations due to its strong octahedral site preference energy. The ratio of Cr^{3+}/Cr^{2+} in the melt is dependent on the oxygen fugacity: nearly all of the Cr in the Fe-bearing system is Cr^{3+} at QFM buffer, while 80% of the Cr is Cr^{2+} at IW buffer (Hanson and Jones, 1997). This means Cr^{3+} available for chromite crystallization is only 20% of the total chromium in the lunar basaltic magma. The lower ratio of Cr^{3+} relative to total Cr combined with the lack of Fe^{3+} in lunar basalts makes the crystallization of chromite more difficult, compared to terrestrial basalts. However, titanian chromite is generally present as a liquidus or near-liquidus phase in the lunar low-Ti and very low-Ti basalts (*e.g.* Papike and Vaniman, 1978), because the Cr content in these basalts are higher than that in the terrestrial basalts (162 ppm in average: Prinz, 1967) roughly by a factor of 10 (BVSP, 1981).

It is to be noted that no chromite was present in the low-pressure equilibrium experiments on the very low-Ti basalt/glass compositions (Grove and Vaniman, 1978; Chen *et al*., 1982) despite the presence of the titanian chromite in the very low-Ti basalts from Apollo 17 and Luna 24 hand specimens (*e.g.* Papike and Vaniman, 1978). In contrast, spinels in the chromite–ulvöspinel solid solutions crystallized both in the hand specimens (*e.g.* Papike and Vaniman, 1978) and the product of the low-pressure equilibrium experiments for the low-Ti basalts (Walker *et al*., 1972, 1976, 1977). Grove and Vaniman (1978) discussed the possibility that the absence of the spinel might result from an error in estimating the Cr_2O_3 content of Luna 24 basalts or lower oxygen fugacity during the experiment relative to the true lunar condition. In addition, the Luna 24 samples might not be representative of the whole rock or basalt flow of the real very low-Ti basalt, since all the known very low-Ti basalt samples are mm-sized fragments found in soils. However, the common absence of spinel in the experiments on the other very low-Ti basalts/glasses rather implies that the missing spinel is a general tendency among the very low-Ti basaltic magma with the compositions currently available. It is worth discussing the effect of Cr content on the spinel crystallization among these very low-Ti basalt, low-Ti basalts, and marginally low-Ti A-881757 basalt, all of which are generated under the similar oxygen fugacity. The Cr contents of the above basalts are listed in Table 10. The low-Ti and very low-Ti basalts in Table 10 are the samples on which compositions the low-pressure equilibrium experiments were conducted. The liquidus or near liquidus chromites crystallized in the low-Ti basalts and they do not in the very low-Ti basalts. As far as the compositions listed in Table 10 are considered, the Cr_2O_3 content in the low-Ti basalts is systematically higher (>0.50 wt%) than that in the very low-Ti basalts (<0.50 wt%). This indicates that the ~0.50 wt% of Cr_2O_3 might be a critical value for chromite precipitation. This implication parallels

Table 10. Cr content (wt%) of lunar low-Ti, very low-Ti basalts, and terrestrial olivine tholeiite.

	Cr_2O_3	Reference
Low-Ti basalts*		
Apollo 12 12002	0.96	1
Apollo 14 14072	0.51	2
Apollo 15 15065	0.50	3
Very low-Ti basalts/glasses**		
Luna 24 24109	0.38	4
Luna 24 24174	0.30	5
Lunar 24 brown glass	0.23	6
Apollo 15 green glass	0.36	6
Apollo17 VLT glass	0.33	7
A-881757	0.17 - 0.29	8, 9
Terrestrial olivine tholeiite	0.05	10

References: (1) Walker *et al.* (1976), (2) Walker *et al.* (1972), (3) Walker *et al.* (1977), (4) Ma *et al.* (1978), (5) Laul *et al.* (1978), (6) Grove and Vaniman (1978), (7) Chen *et al.* (1982), (8) Yanai and Kojima (1991), (9) Warren and Kallemeyn (1993) (10) Hill and Roeder (1974).

* Representative samples in which liquidus chromites are present in low-pressure equilibrium experiments.

** No chromites crystallized in the equilibrium experiments on these basalts/glasses.

with the result of the experiments that the A-881757 basaltic liquid is never saturated with chromite.

Further in the comparison with the terrestrial case, the stability field of the liquidus spinel drastically expands to the lower oxygen fugacity in the experiment of the tholeiite basalt with 500 ppm Cr_2O_3, compared to that with 80 ppm (Hill and Roeder, 1974). Ratio of Cr^{3+} to the total chromium is 20% at IW, and probably less than 20% in the lunar basalt (IW–IW-1) (Hanson and Jones, 1997). If the ratio of Cr^{3+} is assumed to be 10% in the lunar basalt, the abundance of Cr^{3+} available for chromite crystallization in the lunar basalt with 0.5 wt% Cr_2O_3 is comparable to that in the terrestrial basalt with 500 ppm Cr_2O_3. This implication is roughly consistent with the proposed critical value of 0.5 wt% Cr_2O_3 for the chromite crystallization in the lunar basalt. More data on compositions of very low-Ti basalt are required for further discussion on the difference in the spinel crystallization between low-Ti and very low-Ti basalts, and the effect of Cr content on the stability of chromite.

4.4. A-881757 basalt does not represent a primary magma?

The liquidus temperature of A-881757 basalt is as low as 1140°C under the expected oxygen fugacity of lunar magma (IW–IW-1). The liquidus temperature is lower than Apollo low-Ti basalts (T~1300°C) and even a bit lower than Luna 24 very low-Ti basalt (T~1180°C) (Taylor *et al.*, 1991). It is also noted that A-881757 basalt magma is never saturated with olivine, while olivine is on the liquidus for the Apollo low-Ti basalts and pyroclastics (Longhi, 1992). The extremely low liquidus temperature coupled with the paucity of liquidus olivine implies that the composition of the A-881757 basalt may represent a liquid derived from near-surface fractionation processes, where the liquidus

olivine was removed by a gravitational settling in a thick lava flow or shallow magma chamber. This implication parallels with that inferred from its Fe-rich bulk composition (21–23 wt% of FeO) (*e.g.* Yanai and Kojima, 1991; Warren and Kallemeyn, 1993), compared to the Apollo and Luna basalts with similar Ti contents (Taylor *et al*., 1991). Luna 24 very low-Ti basalt with high FeO content comparable to that of A-881757 also lacks liquidus olivine (Grove and Vaniman, 1978).

Chromite is generally an early-crystallizing phase with or without olivine for terrestrial basaltic magmas (*e.g.* Sack and Ghiorso, 1991). The primary magma of the A-881757 basalt could have precipitated chromite very early in the crystallization sequence (possibly as a liquidus phase), during near-surface fractionation prior to the eruption. However, such possibility remains unresolved only with the composition of A-881757 basalt sample at this moment.

Although the A-881757 basalt might not be a primary liquid, the crystallization sequence of pyroxene followed by plagioclase under the oxygen fugacity of lunar magma (IW–IW-1) in the isothermal experiment is consistent with the mineralogical observation of A-881757 basalt (*e.g.* Yanai, 1991; Arai *et al*., 1996). This shows that the experiments on the A-881757 composition could reproduce the crystallization sequence of the A-881757 basalt hand specimen, at least with respect to the major silicate phases. Furthermore, the chromian ulvöspinels produced in the cooling experiment successfully demonstrated that they crystallized in the evolved liquid of the A-881757 basalt magma as a result of the extensive fractional crystallization.

5. Conclusions

(1) A series of isothermal experiments on a lunar meteorite A-881757 basalt composition showed that the A-881757 basalt magma is not saturated with chromite under the expected lunar oxygen fugacity condition (IW–IW-1).

(2) A peritectic reaction among chromite, melt, and pyroxene is present for A-881757 basalt magma under the oxygen fugacity condition one or two log unit higher than the lunar condition.

(3) The cooling experiment successfully reproduced the chromian ulvöspinels with similar compositions to those in A-881757.

(4) The result of cooling experiments further implies that chromites would never precipitate during entire crystallization sequence, and chromian ulvöspinels crystallized solely from highly-fractionated interstitial melts in the late stage of crystallization.

(5) The disparity in the crystallization of liquidus chromite between low-Ti and very low-Ti basalts may reflect the difference of bulk Cr_2O_3 concentration.

(6) The low liquidus temperature and the paucity of liquidus olivine in A-881757 imply that the A-881757 basalt likely represents a liquid derived from near-surface fractionation processes. Chromites might possibly have crystallized during that near-surface fractionation episode prior to the eruption of the magma.

Acknowledgments

We are greatly indebted to Prof. Ikuo Kushiro of Japan Agency for Marine-Earth

Science and Technology for his guidance on the experiment and the productive discussion. We wish to thank Dr. Bjorn Mysen of the Geophysical Laboratory of the Carnegie Institution of Washington for providing us with the unpublished data of Shuart and Muan. We also thank Drs. Katsura Kobayashi and Yoshiyuki Iizuka of Institute for Study of the Earth's Interior, Okayama University for their useful discussions and technical supports. Thorough and constructive reviews by Drs. Naoya Imae, and Takashi Mikouchi are gratefully acknowledged. We thank Dr. Gordon McKay for his helpful review.

References

Akella, J., William, R.J. and Mullines, O. (1976): Solubility of Cr, Ti and Al in coexisting olivine, spinel and liquid at 1 atm. Proc. Lunar Sci. Conf., **7th**, 1179–1194.

Arai, T., Takeda, H. and Warren, P.H. (1996): Four lunar mare meteorites: Crystallization trends of pyroxene and spinels. Meteorit. Planet. Sci., **31**, 877–892.

Barnes, S.J. (1986): The distribution of chromium among orthopyroxene, spinel and silicate liquid at atmospheric pressure. Geochim. Cosmochim. Acta, **50**, 1889–1909.

BVSP (Basaltic Volcanism Study Project) (1981): Basalts as probes of planetary interiors: Constraints from major and trace element chemistry. Basaltic Volcanism of the Terrestrial Planets, New York, Pergamon Press, 311–336.

Chen, H.-K., Delano, J.W. and Lindsley, D.H. (1982): Chemistry and phase relations of VLT volcanic glasses from Apollo 14 and Apollo 17. Proc. Lunar Planet. Sci. Conf., **13th**, A171-A181 (J. Geophys. Res., **87** Suppl.).

Fisk, M.R. and Bence, A.E. (1979): Experimental studies of spinel crystallization in FAMOUS basalt 527-1-1. EOS; Trans. Am. Geophys. Union, **60**, 420.

Grove, T.L. and Vaniman, D.T. (1978): Experimental petrology of very low TI/VLT basalts. Mare Crisium: The View from Luna **24**. New York, Pergamon Press, 445–471.

Hanson, B. and Jones, J.H. (1997): The effect of Fe on Cr redox state in spinel-saturated basalts. Lunar and Planetary Science XXVIII. Houston, Lunar Planet. Inst., Abstract #1678 (CD-ROM).

Hill, R. and Roeder, P. (1974): The crystallization of spinel from basaltic liquid as a function of oxygen fugacity. J. Geol., **82**, 709–729.

Huebner, J.S., Lipin, B.R. and Wiggins, L.B. (1976): Partitioning of chromium between silicate crystals and melts. Proc. Lunar Sci. Conf., **7th**, 1195–1220.

Irvine, T.N. (1965): Chromian spinel as a petrogenetic indicator, part 1. Petrologic applications. Can. J. Earth Sci., **2**, 648–672.

Irvine, T.N. (1967): Chromian spinel as a petrogenetic indicator, part 2. Petrologic applications. Can. J. Earth Sci., **4**, 71–103.

Kushiro, I. and Haramura, H. (1971): Major element variation and possible source materials of Apollo 12 crystalline rocks. Science, **171**, 1235–1237.

Kushiro, I., Nakamura, Y. and Akimoto, S. (1974): Petrological and mineralogical studies on Apollo-12 crystalline rocks: a preliminary report. Mineral. Soc. Jpn. Spec. Pap., **1**, 13–17.

Laul, J.C., Vaniman, D.T. and Papike, J.J. (1978): Chemistry, mineralogy and petrology of seven >1 mm fragments from Mare Crisium. Mare Crisium: The View from Luna 24. New York, Pergamon Press, 537–568.

Lipin, B.R. and Muan, A. (1975): Equilibrium relations among iron-titanium oxides in silicate melts: The system $CaMgSi_2O_6$–"FeO"–TiO_2 in equilibrium with metallic iron. Proc. Lunar Sci. Conf., **6th**, 945–958.

Lofgren, G.E., Donaldson, C.H., Williams, R.J., Mullin, O., Jr. and Usselman, T.M. (1974): Experimentally reproduced textures and mineral chemistry of Apollo 15 quartz normative basalts. Proc. Lunar Sci. Conf., **5th**, 549–567.

Longhi, J. (1992): Experimental petrology and petrogenesis of mare volcanics. Geochim. Cosmochim. Acta, **56**, 2235–2251.

Ma, M.-S., Schmitt, R.A., Nielsen, R.L., Taylor, G.J., Warner, R.D., Lange, D. and Keil, K. (1978): Chem-

istry and petrology of Luna 24 lithic fragments and $<250\,\mu$m soils: Constraints on the origin of VLT mare basalts. Mare Crisium: The View from Luna 24. New York, Pergamon Press, 562–592.

Misawa, K., Tatsumoto, M., Dalrymple, G.B. and Yanai, K. (1993): An extremely low U/Pb sources in the Moon: U-Th-Pb, Sm-Nd, Rb-Sr, and ^{40}Ar-^{39}Ar systematics of lunar meteorite Asuka 881757. Geochim. Cosmochim. Acta, **57**, 4687–4702.

Miyamoto, M. and Mikouchi, T. (1996): Platinum catalytic effect on oxygen fugacity of CO_2-H_2 gas mixtures measured with ZrO_2 oxygen sensor at 10^5 Pa from 1300 to 700℃. Geochim. Cosmochim. Acta, **60**, 2917–2920.

Muan, A., Hauck, J., Osborn, E.F. and Schairer, J.F. (1971): Equilibrium relations among phases occurring in lunar rocks. Proc. Lunar Sci. Conf., **2nd**, 497–505.

Muan, A., Hauck, J. and Löfall, T. (1972): Equilibrium studies with a bearing on lunar rocks. Proc. Lunar Sci. Conf., **3rd**, 185–196.

Nyquist, L.E. and Shih, C.-Y. (1992): The isotopic record of lunar volcanism. Geochim. Cosmochim. Acta, **56**, 2213–2234.

Papike, J.J. and Cameron, M. (1976): Crystal chemistry of silicate minerals of geophysical interest. Rev. Geophys. Space Phys., **14**, 37–80.

Papike, J.J. and Vaniman, D.T. (1978): Luna 24 ferrobasalts and the mare basalt suite: Comparative chemistry, mineralogy, and petrology. Mare Crisium: The View from Luna 24. New York, Pergamon Press, 371–401.

Prinz, M. (1967): Geochemistry of basaltic rocks: trace elements. Basalt, the Poldervaart Treatise on Rocks of Basaltic Composition, ed. by H.H. Hess and A. Poldervaart. New York, Interscience Publ., 271–323.

Sack, R.O. and Ghiorso, M.S. (1991): Chromian spinels as petrogenetic indicators: Thermodynamic and petrological applications. Am. Mineral., **76**, 827–847.

Sato, M. (1978): Oxygen fugacity of basaltic magmas and the role of gas-forming elements. Geophys. Res. Lett., **5**, 447–449.

Sato, M., Hickling N.L. and McLane, J.E. (1973): Oxygen fugacity values of Apollo 12, 14, and 15 lunar samples and reduced state of lunar magmas. Proc. Lunar Sci. Conf., **4th**, 1061–1099.

Schreiber, H.D. and Haskin. L.A. (1976): Chromium in basalts: Experimental determination of redox states and partitioning among synthitic silicate phases. Proc. Lunar Sci. Conf., **7th**, 1221–1259.

Schreifels, W.A. and Muan, A. (1975): Liquid-solid equilibria involving spinel, ilmenite, and ferropseudobrookite in the system "FeO"–Al_2O_3–TiO_2 in contact with metallic iron. Proc. Lunar Sci. Conf., **6th**, 973–985.

Takeda, H., Arai, T. and Saiki, K. (1993): Mineralogical studies of lunar meteorite Yamato-793169, a mare basalt. Proc. NIPR Symp. Antarct. Meteorites, **6**, 3–13.

Tatsumoto, M., Knight, R.J. and Doe, B.R. (1971): U-Th-Pb systematics of Apollo 12 lunar samples. Proc. Lunar Sci. Conf., **2nd**, 1521–1546.

Taylor, G.J., Warren, P.H., Ryder, G., Delano, J., Pieters, C. and Lofgren, G.E. (1991): Lunar rocks. Lunar Sourcebook—A User's Guide to the Moon, ed. by G.H. Heiken *et al*. Cambridge, Cambridge Univ. Press, 183–284,

Walker, D., Longhi, J. and Hays, J.F. (1972): Experimental petrology and origin of Fra Mauro rocks and soil. Proc. Lunar Sci. Conf., **3rd**, 797–817.

Walker, D., Kirkpatrick, R.J., Longhi, J. and Hays, J.F. (1976): Crystallization history of lunar picritic basalt sample 12002: Phase equilibria and cooling rate studies. Geol. Soc. Am. Bull., **87**, 646–656.

Walker, D., Longhi, J., Lasaga, A.C., Stolper, E.M., Grove, T.L. and Hays, J.F. (1977): Slowly cooled microgabbro 15555 and 15065. Proc. Lunar Sci. Conf., **8th**, 1521–1547.

Warren, P.H. and Kallemeyn, G.W. (1993): Geochemical investigation of two lunar mare meteorites; Yamato-793169 and Asuka-881757. Proc. NIPR Symp. Antarct. Meteorites, **6**, 35–57.

Yanai, K. (1991): Gabbroic meteorite Asuka-31: Preliminary examination of a new type of lunar meteorite in the Japanese collection of Antarctic meteorites. Proc. Lunar Planet. Sci. Conf., **21**, 317–324.

Yanai, K. and Kojima, H. (1991): Variety of lunar meteorites recovered from Antarctica. Proc. NIPR Symp. Antarct. Meteorites, **4**, 70–90.